




Phantom illusion based vibrotactile rendering of affective touch patterns

Robert Kirchner , Robert Rosenkranz , Brais Gonzalez Sousa , Shu-Chen Li , and M. Ercan Altinsoy .

Abstract—Physically accurate (authentic) reproduction of affective touch patterns on the forearm is limited by actuator technology. However, in most VR applications a direct comparison with actual touch is not possible. Here, the plausibility is only compared to the user's expectation. Focusing on the approach of plausible instead of authentic touch reproduction enables new rendering techniques, like the utilization of the phantom illusion to create the sensation of moving vibrations. Following this idea, a haptic armband array (4x2 vibrational actuators) was built to investigate the possibilities of recreating plausible affective touch patterns with vibration. The novel aspect of this work is the approach of touch reproduction with a parameterized rendering strategy, enabling the integration in VR. A first user study evaluates suitable parameter ranges for vibrational touch rendering. Duration of vibration and signal shape influence plausibility the most. A second user study found high plausibility ratings in a multimodal scenario and confirmed the expressiveness of the system. Rendering device and strategy are suitable for a various stroking patterns and applicable for emerging research on social affective touch reproduction.

Index Terms—Affective touch reproduction, phantom illusion, vibrotactile feedback, haptic display, haptic rendering

I. INTRODUCTION

ONGOING digitization enables the transfer of many activities into a virtual or augmented reality. This development towards virtual environments (VE) could be voluntary, e.g. to enable higher productivity in work environments or full immersion gaming experiences. Alternatively, it could be involuntary through circumstantial constraints like homeschooling during the pandemic or long distance relationships. To create authentic experiences, much effort is taken to improve the visual modality of the immersion in virtual environments. While in some cases, the haptic modality might only be an add-on, in others it is a primary channel of sensation [1]. During the pandemic, social distancing and homeschooling resulted in gross reductions of direct daily social contacts.

The authors acknowledge the financial support by the Federal Ministry of Education and Research of Germany in the programme of "Souverän. Digital. Vernetzt.". Joint project 6G-life, project identification number: 16KISK001K. This work was supported by the IEEE Technical Committee on Haptics of the IEEE Robotics and Automation Society under the Innovation in Haptics award grant. Funded by the German Research Foundation (DFG, Deutsche Forschungsgemeinschaft) as part of Germany's Excellence Strategy – EXC 2050/1 – Project ID 390696704 – Cluster of Excellence "Centre for Tactile Internet with Human-in-the-Loop" (CeTI) of Technische Universität Dresden.

R. Kirchner, R. Rosenkranz, M. E. Altinsoy are with the research cluster 6G-life, Chair of Acoustic and Haptic Engineering, Technische Universität Dresden, 01062 Dresden, Germany e-mail: robert.kirchner1@tu-dresden.de.

B. G. Sousa, S.-C. Li are with the research cluster 6G-life, Chair of Lifespan Developmental Neuroscience, Technische Universität Dresden, 01062 Dresden, Germany.

R. Rosenkranz, S.-C. Li, M. E. Altinsoy are further with the Centre for Tactile Internet with Human-in-the-Loop (CETI).

This missing social interaction with others poses a risk for the healthy development of children and young adults [2]. Although a technical solution cannot replace real human interactions, digital actuation of social touch could help, when a real touch is not possible. While headphones and head mounted displays enable almost authentic visual and auditory stimuli, technological solutions for creating authentic, i.e. physically accurate haptic sensations, is extremely challenging. This is due to the complexity of touch interactions. Being touched or touching objects usually includes dynamic components, such as movements over the skin, as well as onset and ending of touch. In addition, other cues like temperature, force, contact area, just to name a few, add on to one perception we perceive as touch [3]. Reproducing all of these factors physically accurate would demand bulky mechanisms and heavy equipment and has therefore not been done yet with wearable devices.

According to [4] there are two types of illusion that mediate if a user interacts with an virtual environment as with an real environment: the place illusion and the plausibility illusion. If both are elicited, the user perceives and interacts as in the real world. A convincing subjective perception of place in VE relies on the user to have the feeling of being in a real place, which depends on factors like latency and display resolution. The subjective perception of the experienced virtual scenery being plausible depends on whether the virtual experience is in accordance with the user's expectations. Compared to the place illusion, the plausibility illusion has received little attention [4]. Producing this feedback is possible via authentic or plausible approach [5]. The approach to evoke the same perceptions in the VE as in the related real environment is the authentic approach. Unfortunately, it demands quasi physically accurate reproduction, exceeding widely available haptic reproduction hardware capabilities. The plausible approach, on the other hand, is to create perceptions in the VE that could have occurred in a comparable real environment [5]. This implies that any perceived stimulus that is similar to reality can be utilized, as long as it matches the user expectations. Since every stimulus, fulfilling the expectations, is suitable, it becomes possible to choose the one implying the lowest demand on the reproduction system to reproduce.

In most virtual reality scenarios the users cannot directly compare their percepts to the corresponding real environment, but have to rely on their expectations regarding the depicted situational context. Therefore, the user compares the elicited perceptual properties with relevant expected ones in order to decide whether the presented haptic stimulus is plausible. Thus, the plausible approach has many advantages and is a

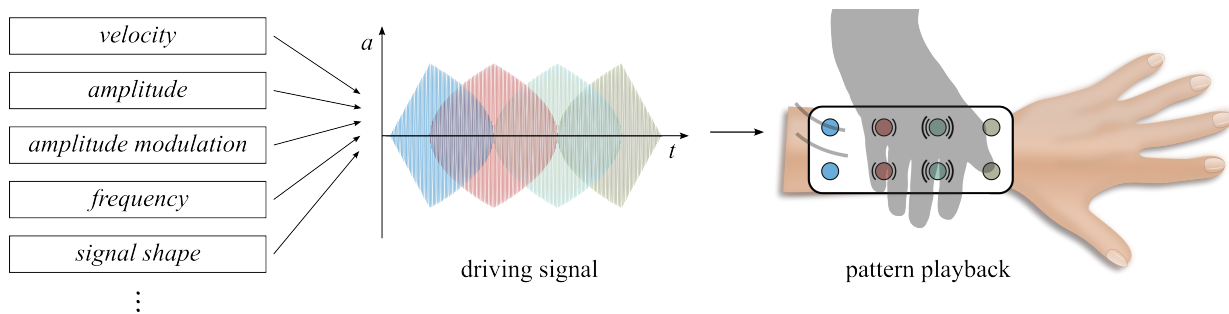


Fig. 1. Sketch of functional principle of the system. With set parameters, multichannel signals can be calculated that correspond to a touch pattern and which can be played by the armband device.

promising approach. It enables perceptual substitution as a tool to derive simplified and reproducible feedback.

In terms of touch reproduction, it is therefore unnecessary to accurately reproduce every aspect of a touch in order for the reproduction to be plausible. To meet the user expectation of stroking the forearm with the hand, it might be sufficient, for example, to simply create a movement sensation on the arm that follows the same movement pattern as the hand. A vibration moving continuously over the arm could thus create an illusion of this stroking movement. Despite using vibration instead of a static pressure, it could elicit a convincing or similar perception thanks to the matching movement pattern. If the user then compares this perception with his or her expectation, he or she could regard the feedback as plausible.

This is especially important since actuating an authentic moving static pressure (as present in a stroke over the arm) requires bulky and not wearable devices [6]. Zhu et al. have demonstrated the use of voice coil actuators in very low frequencies, which come close to a static touch pressure [7]. While this approach achieves higher “realness” for touch patterns like poking and squeezing, stroking patterns were very limited in speed variety. By utilizing vibration, vibrational haptic illusions can be used to achieve arbitrary movement patterns. The plausible approach can thus lower the requirements for the playback systems and at the same time allow the usage of perceptual illusions that enhance playback capabilities.

This work presents on a novel rendering strategy for social affective touch patterns. By utilizing state of the art hardware with limited capabilities, we propose a haptic rendering system, consisting of an armband device for the forearm (4×2 actuator array) and a driving rendering algorithm (outlined in Fig.1) to generate plausible vibrational feedback for affective touch in VE. We chose the forearm, as many different affective touch patterns are executed here and it is easily accessible. As well, it is one of the body parts with the highest acceptance of touch [8]. Touch cues on the forearm have therefore been of particular interest of researchers [9], [10]. With this paper, we aimed to give insights into the development and functionality of the armband device. Further, we determined optimal parameter settings in a perception study of stroking, which is the most referenced affective touch movement over the forearm. The decisive factors thereby are plausibility and continuity of the vibrational playback. Lastly, we evaluated the capabilities of our rendering system in a multimodal experiment with

visual and haptic stimuli in order to achieve a more close to application evaluation.

II. RELATED WORK

A. Affective touch reproduction

Affective touch reproduction is not only important in VE, but also plays an important role in the field of affective touch in psychology and neuroscience [11], [12]. In experimental setups in these fields of research, the touch is commonly reproduced by the stroking of a brush over the participant’s skin [13], [14]. Thereby the experimenter has to reproduce this stroking movement as equal as possible for every participant. The affective velocity of this stroking movement lies in the range of $3 \dots 10 \text{ cm s}^{-1}$ [15]. To compare those affective speeds with non-affective (discriminative) speeds the overall range of velocities in such experiments usually varies from $0.5 \dots 30 \text{ cm s}^{-1}$ [16]. Besides the reproduction of the velocity and trace, also the appropriate onset timing and pressure have to be applied. There have been investigations to automate the application of the brush strokes (e.g. [6]) but those systems are not widely available and not portable or even wearable. Therefore, many experiments are still carried out by hand stroking. This can cause deviations in the repetitions in experiments, which then can lead to uncertainties in the experiment results. Having a widely available system to automate stroking sensations similar to a stroke of a brush could therefore open new possibilities for research in the aforementioned fields.

During the development of devices for rendering affective haptic stimuli, approaches have been investigated at various sites on the body with a variety of different working mechanisms [17]–[27]. Specifically for the forearm, different systems were investigated, mainly with vibration [16], [28]–[30]. Recent developments have focused more on slow to static pressure cues, actuated by shape memory alloys [31], linear actuators [32], pneumatic actuators [33] or voice coil actuators [7], [34]. The objective of the latter investigations was to achieve a more authentic reproduction in comparison to vibration. However, the gain in authenticity was accompanied by a limitation in versatility compared to the vibratory approaches. Especially two-dimensional stroking motions have not been demonstrated yet with those systems. Vibrational illusions on the other hand enable arbitrary continuous movement patterns also in 2D [30] and are thus a

versatile choice for stroking touch reproduction. Furthermore, because of this lack of vibrational illusions, static pressure haptic displays have a discrete resolution, namely the distance of the actuators. For vibrations on the other hand, this is not the case as [30] demonstrated a haptic display with continuous resolution, which is enabled by the vibrational phantom illusion (see following chapter).

Mediated social affective touch devices can be used to directly transmit emotions through haptic patterns [27], [30], [35], [36] and/or to reproduce the touch pattern itself [7], [27], [28], [34]. The former is usually done in the haptic modality alone, without any visual context. While it is an interesting question whether haptics alone can convey emotions, in applications like VE, visual and audio stimuli, as well as social factors are usually present. Research has shown that this context can influence the haptic perception [37] as well as the perception of affectivity and pleasantness [38]. For example, [39] has shown that a visual representation with head mounted displays alone, can change the perception of a vibration path from straight to curved and vice versa. Due to this strong influence on the affective perception by the other modalities, we focus on the reproduction of just the touch pattern itself, without any tuning in order to achieve clearer emotional meaning. [38] underlined the use of the haptic modality to assist the other modalities.

Recent work of McIntyre et al. [40] and Maallo et al. [9] shows, that emotional meanings of affective touch patterns are conveyed by the variation of contact area, normal velocity and tangential velocity. This implies that a reproduction device should be able to render these parameters in order to achieve a plausible reproduction in a scenario where such a pattern is executed in VE. Aside from rendering these parameters, also the vibration signal parameters need investigation. To the best of our knowledge, neither the influence of the letter, nor suitable settings for them have been investigated yet in regards to plausible touch reproduction. Previous approaches to 2D touch pattern reproduction were based on recordings of real touches [7], [28], [35]. Therefore, a rendering strategy to generate such touch patterns by computer is still missing. As a result, an application in VR with devices from the mentioned works does not seem possible without further ado. Due to a necessary selection or post-processing of the recordings, live human-to-human mediated touch via sensor and actuator armbands has not yet been demonstrated. These problems of pattern generation and live rendering can be solved by parameterizing the touch patterns themselves. This approach of parametric touch pattern description, combined with a rendering strategy that can implement these parameters as vibratory feedback, offers the advantage of fully automatic touch generation. This would enable touch interactions in computer generated environments like VR. An implementation of touch pattern recognition in combination with a sensor armband, could furthermore enable live and direct human-to-human mediated touch. In this way, it can be additionally ensured that the played back touch is optimally transmitted and rendered.

B. Haptic illusions for vibrational movement perception

As aforementioned, affective haptic stimulation involves a multitude of cues on the skin. In the tactile domain, the most important cues in this regard are movement, pressure and texture [34]. In the case of affective touch stroking movements on the skin, a static pressure is only elicited for a short amount of time at a certain position on the skin. For a sufficiently fast movement, it is therefore questionable whether the pressure cue plays such an important role. The fact, that affective touch often involves movements over the skin, demands special strategies to reproduce such moving sensations with fixed actuators (as present in wearables). In this context haptic illusions have been investigated, namely the apparent movement illusion (AMI) [16], [41], [42] and the phantom illusion (PI) (also called sensory funneling illusion) [30], [43], [44]. The principles of usage for these illusions of AMI and PI are very well described in [41] and [44] respectively, as well as in [45]. By using at least 3 actuators for the PI, 2-dimensional movement patterns become available. Combinations of both illusions are possible as well, which enables 2D vibrational patterns also for AMI [41], [42]. It should be mentioned that, to the best of our knowledge, the usability for 2-dimensional movement patterns (beyond the proof of concept) was only demonstrated for PI so far in [30].

There are some differences in the capabilities of the two illusions. The AMI has a narrow control range in which different velocities can be rendered [46]. The PI on the other hand has practically no limitations in stroking velocity. It is also possible to change velocities freely during the stroke, up to a full stop. In the context of touch reproduction, the AMI in combination with PI is able to render movements of constant speed with sequential activation of actuators. The PI alone, on the other hand, is able to deliver a continuous tactile display, on which moving and non-moving vibrations can be rendered at arbitrary positions and speeds. Although there apparently has been no direct comparison of the perceived continuity between AMI and PI in a comparable setup published yet, a continuous crossfade of two actuators as done for the PI appears to have a higher potential of continuity in comparison to a pulsing of the actuators as done for AMI. This presumption was further substantiated through informal testing by the authors.

III. THE HAPTIC ARMBAND ARRAY

A. Concept

The haptic armband array device is designed to render haptic affective touch on the forearm. The goal of the design was to enable the rendering of movement and texture cues. The aim was a device that is able to flexibly reproduce different vibrational touch patterns. Finding rendering limitations for the device was an important research question for us. In order to investigate larger parameter ranges, we assured independent and flexible control of intensity, as well as a wide bandwidth of excitable frequencies. Another objective was to create the sensation of continuous movement of the vibrations, while also allowing the rendering of variable velocities and curved paths. For this purpose, an array of actuators was defined, which is operated using the algorithm proposed by Schneider

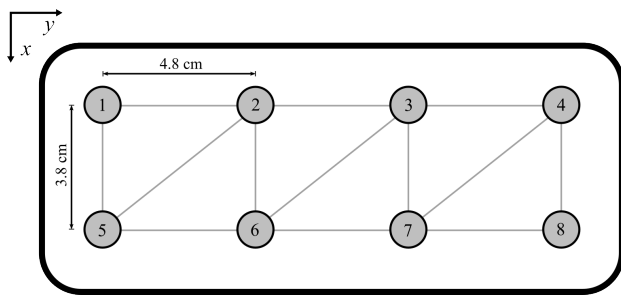


Fig. 2. Schematic drawing of the armband array. Numbered circles mark the positions of the actuators. Grey lines show the subdivision of the area in triangles for the algorithm.

et al. for direct manipulation of tactile grids [44] and thereby utilizing the PI. With it, it is necessary to control each actuator individually. The rendering algorithm was implemented in Matlab. By entering signal shape, movement path of the vibration point, amplitude, velocity and amplitude modulation, the script calculates the vibration strengths of the actuators and finally the signals of the individual actuators. For the signal shape one can choose between sinusoidal oscillations, noise or a combination of both. In principle, however, any playable signal is possible. In this concept, the vibration intensity serves as a perceptual substitution for the actual touch force (i.e. static pressure). With a variation of the overall vibration intensity (i.e. amplitude modulation) it could be possible to mimic dynamic effects, such as the onset or the lift off of the hand.

The dimensions of the armband were determined by the distance between the actuators, which in turn were taken from [47]. It was ensured that the distance between the actuators in the longitudinal direction and in the circumferential direction were within a secure range for the PI. The diagonal distance between the actuators was chosen to be slightly below the maximum two-point threshold on the forearm (as taken from [47]). We ensured sufficient space between the actuators to eliminate possible interference among each other. The chosen design consists of a grid arrangement with 4×2 actuators. Figure 2 shows a schematic of the armband. The distances in the longitudinal direction (y) are 4.8 cm, in the circumferential (x) direction 3.8 cm, and in the diagonal direction 6.1 cm. To prevent transmission of vibration through the armband along the arm, a stretchable fabric was chosen.

For the algorithm, the array is divided into triangles to apply the calculation of barycentric coordinates in the two-dimensional case. Given a motion path for the vibration, the associated relative amplitudes of the actuators can then be calculated for each point on the surface so that the vibration is perceived at that point. Additionally, a one-dimensional case was implemented. In this case only the y -coordinate is used for the calculation according to the principle to calculate a phantom vibration in between two actuators as described in [41]. The calculated relative amplitudes of the actuators can then be applied equally to the actuators that are adjacent in the x -direction. In this way, a PI is induced again, so that the vibration is perceived along the center of the armband.

For the calculation of the vibration intensity in both the 1D and 2D cases a quadratic (also named "Power" in [41]

and [44]) interpolation is used, although linear and logarithmic are also implemented. This method causes a more continuous sensation, i.e. a more evenly perceived vibration intensity compared to linear and logarithmic interpolation in informal prior testing.

Initially the algorithm generates the vibration signal with the desired amplitude, waveform and amplitude modulation. Assuming a constant velocity, the signal duration T is calculated from a linear fade-in and fade-out, each with a duration $T_{\text{fade in}} = T_{\text{fade out}} = 0.6$ s plus the duration of the motion according to:

$$T = T_{\text{fade in}} + d/v + T_{\text{fade out}} \quad (1)$$

with the distance d between the start and endpoint of the motion and the velocity of the motion v . The fade-ins and -outs are necessary, since the actuator needs a certain time to rise to full amplitude. If this would not be taken care of, the amplitude of the first actuator would already decrease (caused by the moving vibration) before it could reach its initial maximum. Then the amplitude modulation is computed for every point of time according to:

$$a_{\text{mod}}(t) = a_{\text{nomod}}(t) \left(\left(1 - \frac{m}{2}\right) - \frac{m}{2} \cos(2\pi f_m t) \right) \quad (2)$$

where $a_{\text{mod}}(t)$ is the amplitude of the modulated signal of a certain point of time t , $a_{\text{nomod}}(t)$ is the amplitude of the unmodulated signal, m is the modulation index, and f_m is the modulation frequency. Next, the relative amplitudes of the actuators are calculated for all points along the motion path and stored as gain factors. The points along the curve are derived from the subdivision of the motion into arbitrarily small time steps. For each time step, this produces an amplification factor for each actuator, by which a part of the signal for the corresponding time step is multiplied. This results in 8 actuator-specific signal traces, which correspond to an actuator-specific amplitude modulation of the signal. Figure 3 shows the temporal progression of the signals for a movement along an actuator row. At the end of the calculation, an 8-channel audio file is generated, which contains the signals for each actuator.

In the application (e.g. our user study), the audio files are read in again and the contained signals are played as vibrations over an audio output of a sound card. For testing purposes, a GUI was designed in Matlab which allows the movement of a vibration point with any frequency and amplitude over the arm in real time using a cursor. The position of the virtual vibration point is read out live and the vibration strength of the actuators is calculated according to the algorithm to render play the vibration at the right position on the arm. According to the sample frequency and buffer size, the vibration playback on the arm is then updated, thus enabling a real-time capability of the system.

B. Components

Lofelt L5 were selected as actuators in our design. These are wide-band LRA, or so-called voice coil actuators, which enable operation in larger frequency ranges. The previously described algorithm calculates the stimuli. These are then

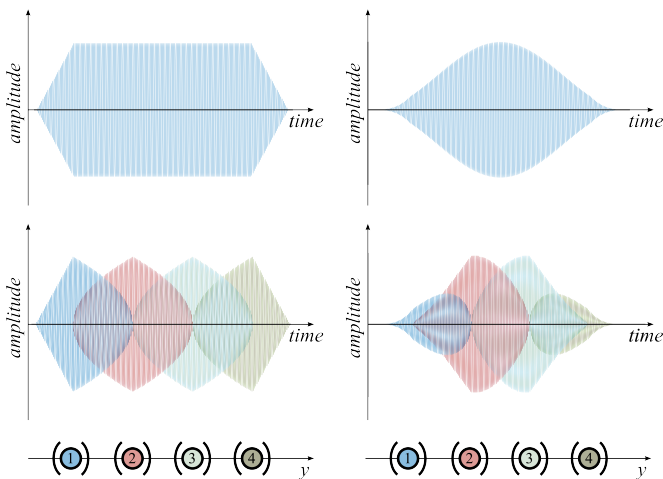


Fig. 3. Illustration of the algorithm output for a uniformly moving vibration (from actuator 1 to actuator 4). The upper plots show the generated signal for the vibration without (left) and with (right) amplitude modulation. The lower plot shows this signal as calculated by the algorithm for every actuator (as indicated by color below) with quadratic interpolation. The signals are displayed in time domain.

read out and passed to a sound card (Fireface UCX, RME), which has 8 outputs. The generated signal is then amplified by an 8-channel audio amplifier (STA-850D, img) and finally transmitted to the individual actuators. Each channel in the signal generation thus has a direct counterpart as an actuator. The actuators are enclosed in 3D printed housings and screwed to the armband. On the bottom of the housing, which faces the skin, a dome-shaped (diameter about 10 mm and height about 4 mm) silicone knob is attached. This ensures a good coupling of the vibration into the skin. The predominant direction of vibration is in the direction of the longitudinal axis of the arm (y -direction), as marked in Fig. 4. The acceleration in the other dimensions of the actuator are at least 15 dB lower and are therefore assumed to be negligible in this work.

C. Calibration

To be able to generate stimuli at a defined acceleration level, the signal chain was calibrated. For this purpose, the transfer function of the actuator (when worn with the armband on the forearm) was measured with white noise. The gain on the amplifier was chosen for operation and calibration in a manner that the maximum possible signal was within the allowable limits of the vibration motors. To compensate for the transfer function, filter coefficients were calculated which are used to apply a FIR (finite impulse response) filter to the calculated signal from the stimuli. The accuracy of the acceleration amplitude level of the calibrated system is about ± 3 dB. With the just noticeable difference being 3 dB (45 %) [48] it is therefore considered to be sufficiently accurate.

IV. ASSESSING OPTIMAL SIGNAL PARAMETERS FOR TOUCH PATTERNS

A user study was conducted to assess the playback capabilities of the armband with respect to a simple touch movement, i.e., stroking the forearm with the hand. The main purpose was



(a) Outside of the armband

(b) Inside of the armband

Fig. 4. Armband with actuator housing, wiring and predominant direction of vibration (arrows) of the actuator array in (a). Backside of the housing with silicone knob (10 mm diameter, 4 mm height) that provides skin contact in (b).

to assess the performance of the algorithm and the actuator array for generating continuous movements and to find limits for the playback parameters. Thus, the goal of the exploratory study was to find favorable parameters that allow for the most plausible rendering of stroking. Our hypotheses in this regard were, first, that the armband is capable of generating continuous motion of vibration with consistent intensity if the signals are designed accordingly to the algorithm. The second hypothesis was that changes in the signal properties have an impact on the perception of the plausibility and the pleasantness of the actuated touch movement.

The necessary generation of the vibratory playback patterns was performed using the algorithm described above. The patterns consisted of a swiping up and down the entire length of the armband. The movement takes place in 1D, as this experiment is intended to demonstrate the feasibility of the algorithm, as well as to determine the influence of signal properties on perception. For the generation of the stimuli, the velocity, amplitude modulation, intensity, and waveform were varied. The slow (3 cm s^{-1}) and fast (10 cm s^{-1}) velocity for affective touch, and one velocity for non-affective touch (18 cm s^{-1}) were set as constant velocities [15]. After informal tests of our own, two options were determined for amplitude modulation: no amplitude modulation and amplitude modulation over the entire playback length. The latter has a period equal to the duration of the movement of one stroke in one direction. Therefore, at the beginning and at the end of the motion, the overall amplitude is zero and reaches a maximum in the middle. This should better mimic the onset and uplift of the hand during a stroking movement. Similarly, a comparable pressure curve occurs on the skin. The signal itself was gener-

TABLE I
ACCELERATION AMPLITUDE LEVELS OF THE STIMULI

	50 Hz	100 Hz	150 Hz	bandlimited noise only
low intensity (dB[$\mu\text{m}/\text{s}^2$])	128	128	131	135
high intensity (dB[$\mu\text{m}/\text{s}^2$])	138	138	141	145

ated as pure sine waves, pure white band-limited white noise and a combination of sine and band-limited white noise. The noise was used as a perceptual substitution for the roughness of the skin when brushing over it, as suggested by Alma et al. in [49] and [50]. According to these findings, the sensation of fine textural roughness (“tingling”) can be sufficiently well represented by band-limited noise, which makes the recording of a real signal unnecessary for this case. For sinusoidal signals frequencies (50, 100, 150) Hz were used and for band-limited noise a band of 40...500 Hz was chosen. For the combined signal, the noise was added to the sinusoidal signal. The noise was generated with the same amplitude as the sine. Then the RMS level of the added signal was adjusted to the RMS level of the pure sine to achieve the same perceived intensity. For all combinations of noise and sinusoidal signal, a strong and a weak variant were defined as signal amplitudes. We aimed to realize equally perceived intensities for all high and all low amplitudes (intensities) respectively. To achieve this, the lower intensity was defined to be 4 dB above the perception threshold, so that it is just well perceivable. The high intensity was defined to be 10 dB above the low intensity. In a preliminary study the latter was found to be a suitable value which is strong but not unpleasantly intensive. The sensing thresholds were based on [51]. However, compared to the latter, we use vibrations tangential to the skin. As Alles described in [52], these are better perceivable. This could be due to a larger activation of receptors in the skin by a more widespread excitation with the same contact area. Although the contact area of the actuators is about 0.79 cm^2 , the true excited area is larger. Following the spatial summation theory proposed by Verrillo [53], this results in a decrease of the perception threshold. After informal experiments of our own, the intensities were set to the values listed in Table I. By using 3 velocities (3 cm s^{-1} , 10 cm s^{-1} , 18 cm s^{-1}), 2 amplitude modulations (with, without), 7 signal combinations (3 sine, 3 mixed, 1 noise), and 2 intensities (high, low), we obtain 84 different stimuli. As described before, each stroke includes a fade-in and fade-out of 0.6 s each.

A. Participants

The study sample included 22 participants (6 female, 16 male) at the age from 21 to 37 with an average age of 29. The study was done with written and informed consent of each participant. The study was done in accordance with an approval from the local TU Dresden ethic committee (SK-EK-5012021-Amendment). No participant reported any impairment of sensation on the forearm.

B. Procedures

Before the experiment, the participant took seat in front of a computer screen and signed an informed consent sheet. Afterwards they were asked to put on the armband in such way, that the middle line of the actuator array aligned with the center of the upside of the forearm that they don't use to move the mouse. For all participants, this was their left arm. To ensure fitting distances, the longitudinal actuator spacing was measured and adjusted. It was explained to the participants that the armband was built to replicate touch patterns. It was also explained to them that the experiment was designed to determine the most appropriate parameters to make this touch as plausible as possible. The participants task was then to rate the plausibility of the played stimuli on a continuous semantic differential scale (“not at all”, “slightly”, “moderate”, “quite”, “very”). The scale translates to rating values ranging from 0...100. Besides plausibility, ratings for continuity continuity of the stroking movement and pleasantness of the playback, were also asked on a equivalent scale, as done by [34] and [43]. Special care was taken to explain “plausibility” in contrast to “authenticity”. It was stated that the armband uses vibration and that it would therefore never be able to exactly reproduce the same (i.e. authentic) perception. The term “plausibility” was then explained as to how “similar”, “fitting” and “convincing” the reproduced touch was in regard to the participants expectation of a simple up-and-down-stroke with a finger over the forearm. An extract of the explanation protocol with the exact definition used is included in the supplemental material. Apart from the fact that the armband works with vibration, no further statements were made about how it functions. Subsequently, the participants were fitted with headphones that played pink noise in order to mask any noise from the actuators. Before the experiment, the participants were then able to gain an overview of the extreme cases of the generated stimuli by performing 4 practice trials. The experiment then began, lasting on average about 30 min. Participants were allowed to repeat the stimuli before an evaluation. However, they were encouraged to decide as intuitively as possible based on gut feeling and to repeat the stimuli as seldom as possible. There was no context accompanying the vibration playback other than the GUI of the experiment.

Prior to the experiment, the participants were not given the opportunity to perform the stroking touch with their hand themselves. Thus, they could evaluate the plausibility rating purely on their expectation of a stroke and had no direct comparison. After the trials, the participants answered a verbal questionnaire in which they had to provide information about the continuous sensation and the quality of the PI deception. They were also asked about their personal preferences for how the playback should feel to be more plausible and pleasant.

C. Data analysis

To investigate if stimuli were rated similarly between subscales, ratings on each subscale were averaged for every stimulus across all participants. Thus, obtaining 84 average ratings, that were then correlated via Pearson's correlation

coefficient. Two linear mixed models with plausibility and continuity as dependent variables inspected the influence of parameters on these ratings, separately. Both linear mixed models included the same set of random and fixed effects: a by-participant random intercept, fixed effects for the individual parameters, and all possible fixed effects interactions between parameters. The significant influence of parameters was tested via F-tests using Satterthwaite approximation for degrees of freedom. For significant fixed effects, post-hoc t-tests on differences between estimated marginal means (EMM) were performed adjusting for multiple testing via Bonferroni correction. Statistical analyses were performed in RStudio with R version 4.1.2.

D. Results

Correlation analyses reveal large positive associations between plausibility and continuity ($r(82) = .73, p < .001$), plausibility and pleasantness ($r(82) = .83, p < .001$), and pleasantness and continuity ($r(82) = .63, p < .001$). Therefore, the usage of linear mixed models mainly focused on how playback parameters influenced plausibility and continuity ratings. Due to high correlation with plausibility, pleasantness results are not detailed at this point. All trials with white noise only as signal combination were removed (12 trials per participant) because its inclusion led to rank-deficient models and nonestimable EMMs. Figure 5 shows the absolute values for the signal combinations averaged over the combinations of amplitude modulation. It is visible, that the combinations with noise only were rated worse than with a purely sinusoidal or combined signal.

Linear mixed model identified several parameters that influenced plausibility ratings. Significant fixed effects were present for velocity ($F(2, 1491.0) = 39.69, p < .001$), intensity ($F(1, 1491.0) = 37.09, p < .001$), and signal form ($F(1, 1491.0) = 15.15, p < .001$). However, involvement in significant interactions does not allow for isolated interpretation of these fixed effects. The interaction between intensity and amplitude modulation ($F(1, 1491.0) = 6.19, p = .013$) reveals that without amplitude modulation low intensity trials are rated as more plausible than high intensity trials ($\Delta\text{EMM} = 8.9, t(1491) = -6.07, p < .001$, see Fig. 6a). Signal form showed interactions with three other variables, namely carrier frequency ($F(2, 1491.0) = 6.41, p = .002$), intensity ($F(1, 1491) = 7.89, p = .005$), and velocity ($F(2, 1491.0) = 4.09, p = .017$). Within the high intensity condition, trials were rated as more plausible for sinusoidal signals ($\Delta\text{EMM} = 6.95, t(1491) = 4.74, p < .001$, see Fig. 6b). Across carrier frequency conditions, significant differences between signal forms were only observed in the 150 Hz condition ($\Delta\text{EMM} = 9.29, t(1491) = 5.17, p < .001$, see Fig. 6c). For the interaction between signal form and velocity, signal forms did not differ at velocities of 3 cm s^{-1} , but at 10 cm s^{-1} ($\Delta\text{EMM} = 5.12, t(1491) = 2.85, p = .03$) and 18 cm s^{-1} ($\Delta\text{EMM} = 7.01, t(1491) = 3.9, p < .001$), sinusoidal trials had higher plausibility ratings than trials applying combined signal forms (see Fig. 6d).

The continuity model showed significant fixed effects for velocity ($F(2, 1491.0) = 9.92, p < .001$), inten-

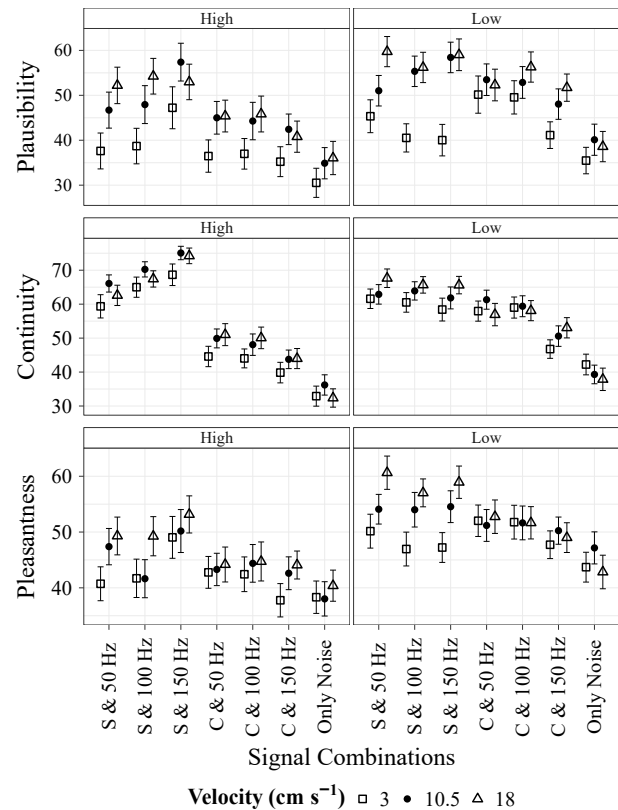


Fig. 5. Ratings of stimuli, averaged over combinations of amplitude modulation. Means of plausibility, continuity and pleasantness ratings are plotted for all combinations of intensity, signal shape (S for sinusoidal and C for combined, i.e. sinusoidal+noise signals), frequency and velocity. The two columns show high (left) and low (right) intensity, respectively. Points give means with \pm standard error as error bars.

sity ($F(1, 1491.0) = 9.21, p = .002$), and signal form ($F(1, 1491.0) = 275.39, p < .001$). However, in comparison to the plausibility model, neither the signal form-velocity interaction ($F(2, 1491.0) = 0.24, p = .786$) nor the amplitude modulation-intensity interaction were significant anymore ($F(1, 1491.0) = 1.03, p = .309$). Additionally, a significant interaction between carrier frequency and intensity ($F(2, 1491.0) = 6.32, p = .002$) revealed that while carrier frequencies did not differ at an high intensity, at a low intensity 150 Hz showed lowest continuity ratings compared to 50 Hz ($\Delta\text{EMM} = 5.34, t(1491) = 3.56, p = .003$) and 100 Hz ($\Delta\text{EMM} = 5.05, t(1491) = 3.37, p = .006$, see Fig. 6e). The significant interaction between signal form and intensity ($F(1, 1491.0) = 68.02, p < .001$) showed reversed trends in continuity ratings across intensities (from high to low intensity) for signalforms. For combined signalforms, a positive linear trend was evident ($t(1491) = 7.98, p < .001$), while for sinusoidal signals a negative linear trend was revealed ($t(1491) = -3.69, p = .006$), see Fig. 6f. The interaction between signal form and carrier frequency ($F(2, 1491.0) = 15.39, p < .001$) revealed that while no differences were detected between carrier frequencies in the sinusoidal condition, in the combined condition, the 150 Hz condition was rated as least continuous (50 Hz – 150 Hz: $\Delta\text{EMM} = 7.23, t(1491) = 4.866, p < .001$; 100 Hz –

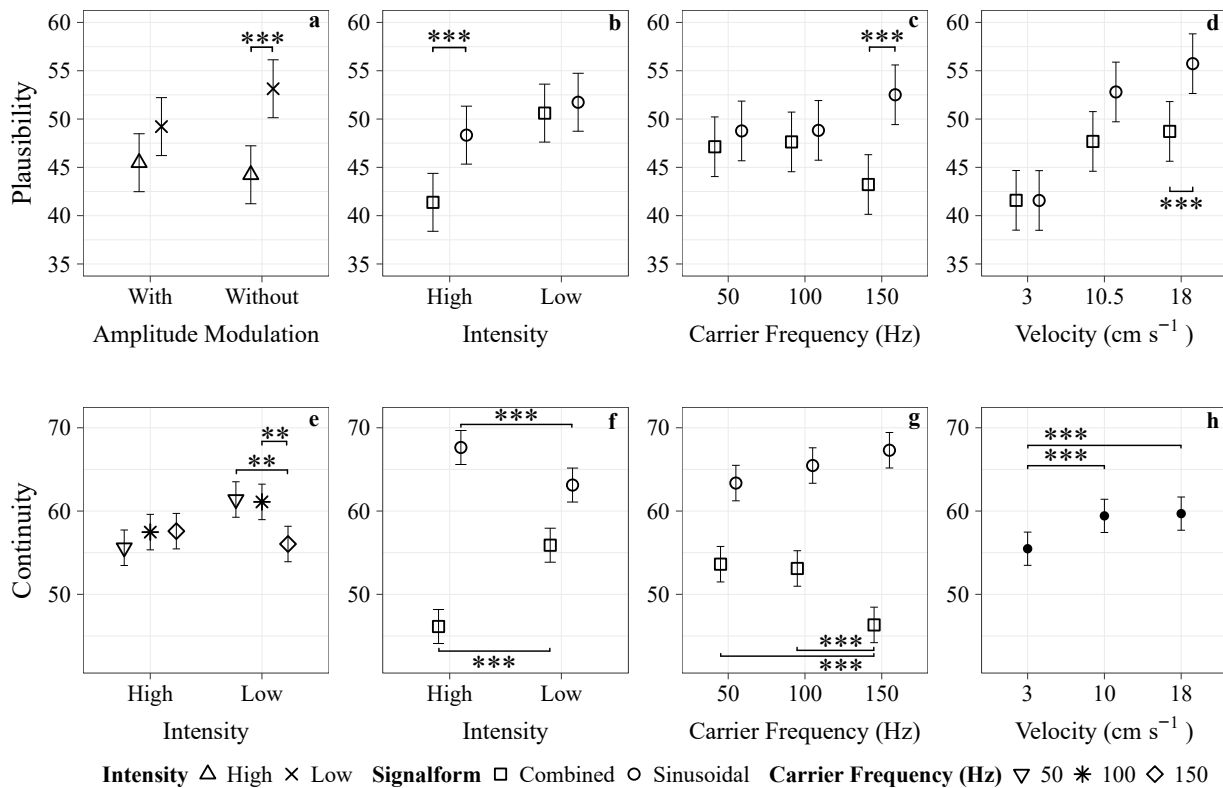


Fig. 6. Plausibility and continuity ratings for playback parameters. Estimates from linear mixed models are plotted for plausibility (upper panel) and continuity (lower panel) ratings. Points give EMMs with \pm standard error as error bars. Interaction effects between the parameter on the x-axis and the parameter plotted with shapes (see legend) are plotted in (a-g). The last plot (h) in the continuity panel shows fixed effects of velocity. Brackets indicate significant pairwise comparisons (a-e and g-h). In (f) brackets denote a positive linear trend for combined versus a negative linear trend for sinusoidal signalforms. $**p < .01$, $***p < .001$.

150 Hz: Δ EMM = 6.77, $t(1491) = 4.522$, $p = .001$), see Fig. 6g. Finally, the fixed effect for velocity showed that 3 cm s^{-1} had lower continuity ratings than both 10 cm s^{-1} (Δ EMM = -3.95 , $t(1491) = -3.72$, $p < .001$) and 18 cm s^{-1} (Δ EMM = -4.21 , $t(1491) = -3.97$, $p < .001$), see Fig. 6h.

V. VALIDATION OF TOUCH PATTERNS IN MULTIMODAL CONTEXT

In order to assess the capabilities of the armband in a closer to application scenario a second user study was conducted. This study served two purposes. Firstly, it should assess the 2D-capabilities of the armband in regards to touch pattern perception by the user. Secondly, it should evaluate a close-to-application plausibility in a multimodal context, i.e. haptic playback with visual context.

For this experiment, 4 different touch patterns were defined, which the armband should reproduce. The patterns consist of a finger stroke over the left forearm. The overall direction of the strokes is towards the wrist. The main difference between the strokes is the finger motion path. There are 3 straight paths and 1 curved path. The straight paths either run on the side or center of the forearm or run diagonal across it. The curved path is a circular arc that starts on the left side ($x = 3.8 \text{ cm}$, runs over to the right ($x = 0 \text{ cm}$) side and ends back on the left side. Fig. 7 shows the four different stroking paths. All

TABLE II
CONSTANT SPEEDS OF TOUCH PATTERNS IN SECOND EXPERIMENT

Central	Curved	Diagonal	Right
5.7 cm s^{-1}	7.9 cm s^{-1}	6.1 cm s^{-1}	5.7 cm s^{-1}

paths start at the $y = 12 \text{ cm}$ and end at $y = 2.4 \text{ cm}$. All strokes have the same duration of 1.7 s. This corresponds to different constant velocities as displayed in Table II. According to the defined stroking paths, matching videos were recorded. In them, a female right hand performs the stroke on a male left forearm. Only the forearms and hands are visible in the videos.

In the experiment, the participants sit in front of a screen. Their left forearm rests straight under a support structure and is covered by a screen. Looking down on the screen from the participant's point of view, the male arm in the video occurs in the same position, as the real left forearm. Fig. 8 shows the experimental setup. The algorithm calculated the vibratory playback patterns for the four strokes with the 2D method. We chose a pure sinusoidal signal with low intensity ($128 \text{ dB}[\mu\text{m/s}^2]$) and no amplitude modulation. According to the first experiment, those settings were the most promising to achieve a maximal level of plausibility. We chose low intensity also because it would better fit a gentle stroke with one finger. Frequency wise, both 100 Hz and 150 Hz produced similarly

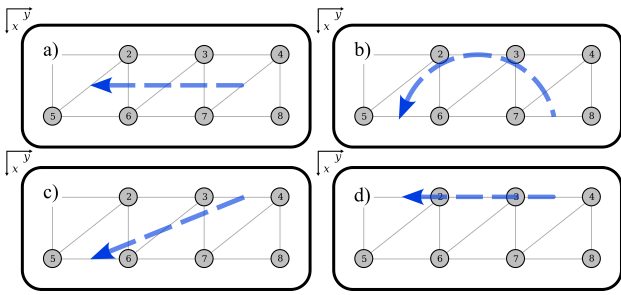


Fig. 7. Schematic drawing of the movement paths in the second experiment: a) central, b) curved, c) diagonal and d) right path. Arrow indicates direction and path of finger/vibration. Top view, actuators 1 and 5 face the hand, actuators 4 and 8 face the elbow.

favorable plausibility ratings. In order to focus the experiment on the two goals stated above and to include more stimuli repetitions, we chose only one frequency, namely 100 Hz to generate the signals. By combining every vibrational touch pattern with every video, we generated 16 different multimodal stimuli. For four of these, the haptic and video touch pattern matched, the others were mismatching combinations (e.g. curved video stroke and right vibrational stroke). All stimuli were timed so that touchdown and lift-off of the hand in the video synchronized with start and end of the vibrational pattern. Each multimodal stimulus was played three times during the experiment. This leads to 48 stimuli in randomized order for the whole experiment. Based on the experiences in the first experiment we built an improved version of the armband. One major drawback of the first armband design was an unwanted change of actuator distance in x -direction due to fabric stretch for different arm sizes. With it, the defined distance could not be ensured and thereby a reliable playback of 2D touch patterns were not possible. We switched from a whole textile sleeve as base to a rectangular textile with velcro stripes for better size adjustability. By using a longitudinally elastic fabric, the actuators stayed decoupled in the dominant direction of vibration. At the same time, the actuator distance in x -direction was fixed due to the very low elasticity of the fabric in said direction. Additionally we eliminated all unwanted noise from the armband, which makes it completely inaudible during operation.

A. Participants

The study sample included 24 Participants (5 female, 19 male) at the age 24 to 60 with an average age of 33. 15 Participants already participated in the first experiment, 9 were naive to the device. The study was done with written and informed consent of each participant. It was conducted in accordance with an approval from the local TU Dresden ethic committee (SK-EK-5012021-Amendment). No participant reported any impairment of sensation on the forearm.

B. Procedures

The Procedure of this second experiment was similar to the first one. The participants took seat in front of a computer screen. This time, the participants had to look down on the



Fig. 8. Photograph of the experimental setup for multimodal context scenes, with participant.

screen which covered their left arm (see Fig. 8). Once the informed consent sheet was signed, the armband was fixed to the left arm of the participant. Then the participants were guided to position their arm in the same place as the arm in the video. With it, the participants gain the same perspective on the arm in the video, as if they were looking directly on their own arm. The experimenter then explained that the purpose of the armband is to reproduce touch patterns. The functionality of the armband was not detailed. The participants were asked to rate the plausibility of the touch playback. In doing so, the term “authentic” was again explicitly distinguished from “plausible”. It was stated that the armband uses vibration and that it would therefore never be able to exactly reproduce the same (i.e. authentic) perception. The term “plausibility” was then explained as to how “similar”, “fitting” and “convincing” the reproduced touch was in regard to the touch in the video. An extract of the explanation protocol is included in the supplemental material. The rating scale was the same semantic differential scale as in the first experiment. Before the experiment, the participants had the chance to accustom in 5 practice trials. Those trials included every video and every touch pattern at least once as well as matching and unmatching combinations. We allowed the repetition of trials to achieve better accuracy. An experiment lasted around 15 min.

As in the first experiment, the participants did not perform a comparable real touch before the experiment. After the experiment, the participants answered three follow-up questions. The first question evaluated the self-perceived difficulty to tell touch patterns apart. The second one asked for aspects in the touch pattern that are missing in order to achieve full plausibility (if not rated to 100). The last question asked for the general ability of the armband to imitate a stroke. We asked the last question to roughly estimate the authenticity of the system.

C. Data Analysis

We carried out a repeated-measures ANOVA (rmANOVA) on the plausibility ratings with haptic- and video-stimuli and their interaction as within-participant factors and participants

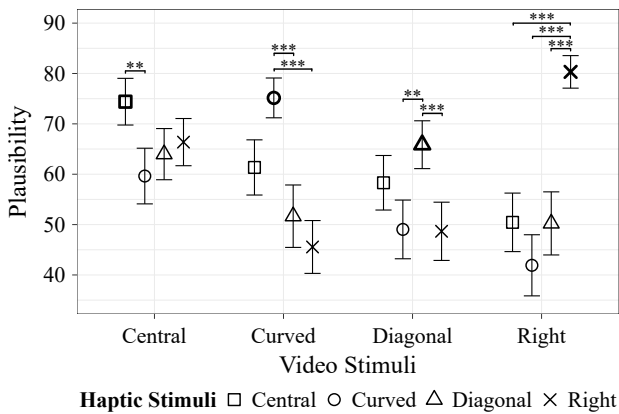


Fig. 9. Plausibility ratings of the second experiment, plotted for all combinations of video and haptic stimuli. Coherent stimuli are highlighted with bold shapes. Points give means with \pm standard error as error bars. Brackets indicate significant post-hoc pairwise comparisons between coherent and incoherent stimuli. $**p < .01$, $***p < .001$.

as error term. To test if coherent haptic and visual input led to higher plausibility ratings, the interaction term of the previous rmANOVA was decomposed into coherent and incoherent components and added to the previous rmANOVA [54], [55]. Additionally, pairwise comparisons for video- and haptic stimuli were performed by controlling for multiple comparisons via Bonferroni correction. Statistical analyses were again performed in RStudio with R version 4.1.2.

D. Results

Fig.9 shows the absolute ratings for each stimuli combination averaged over all participants. For each video the coherent haptic touch pattern achieved the highest rating. The coherent central stimuli average rating was 74.4 with a standard error of ± 4.63 . For curved, diagonal and right coherent stimuli, the ratings were 75 ± 3.95 , 65.9 ± 4.75 and 80.3 ± 3.23 respectively. The rmANOVA on plausibility ratings revealed a significant main effect of video stimuli ($F(3, 1113) = 12.635, p < .001$) and a significant interaction between haptic- and video stimuli ($F(9, 1113) = 23.05, p < .001$). Decomposing the interaction term into coherent and incoherent stimuli, results in a significant coherence term ($F(1, 1113) = 153.93, p < .001$). Post-hoc pairwise comparisons show that coherent stimuli were rated more plausible than the majority of incoherent stimuli. Significant pairwise comparisons from the post-hoc tests are marked in Fig. 9.

VI. DISCUSSION

The aim of the experiments was firstly to prove the functionality of the armband and the signal generation algorithm behind it. Second, the parameter ranges of the stimuli were analyzed in order to determine the playback constraints of the armband on the one hand and to find optimal parameters that maximize the plausibility of the stroking movement on the other hand. Lastly, we evaluated the overall capability of the armband to render 2D stroking in a multimodal context. Proof of functionality could be provided, as none of the participants reported a loss of the illusion. Therefore the

illusion is robust and its limits lie outside of the investigated ranges. Furthermore, it was found that only the speed and the signal shape had significant effects on the plausibility, but not amplitude modulation and frequency of the carrier signal. Intensity showed only a minor influence. This implies, that rendering devices for affective touch patterns have a broader range of design freedom.

The strong correlation between the rating of plausibility and pleasantness shows that the chosen approach to implement the imitation of the touch movements is suitable to produce a non-annoying reproduction. It can therefore be assumed in further studies that an increase in plausibility does not lead to a deterioration of pleasurability, which could have been the case due to an uncanny valley effect in touch reproduction [56]. The plausibility ratings of the first experiment serve mainly to derive parameter influences. Meaningful plausibility ratings for a close-to-application case are provided by the second experiment.

Comparing the different signal forms, pure noise signals have an inferior performance in all three measures, compared to pure sinusoidal and mixed signals. They are therefore not suitable for vibrotactile touch rendering. Combined signals were rated less plausible and less continuous compared to sinusoidal signals, although the effect was stronger on continuity. These findings are in accordance with [57], where sinusoidal signals were perceived more uniform than noisy signals. This suggests a pure sinusoidal signal as the best option to render continuous sensations. Surprisingly, added texture information has either no positive or even detrimental effects on the plausibility ratings. It is therefore sufficient to render sinusoidal vibrations only. Thus, it is possible to merely use narrow bandwidth actuators (i.e. LRA). This simplifies the design of touch reproduction devices. Eccentric rotating mass motors (ERM) could also possibly be used, but it has to be taken into account that while varying their amplitude, their frequency also changes. This could affect the illusion of the PI, as the frequencies of the individual actuators would usually not be the same.

The lower rating of the slow speed could be due to a relatively long movement path corresponding to a longer vibration time (12s compared to 5.14s and 4s for 10 cm s^{-1} and 18 cm s^{-1} , respectively). Hence, it remains unclear, whether the prolonged vibration exposure or the slow speed itself deteriorated the perception of the touch pattern. Adaptation to vibrotactile stimulation is not likely to have affected any ratings. The average vibration duration with an acceleration level above the non adaptation threshold for each actuator in the longest stimuli was below 2s for both experiments. In comparison, relevant vibration durations for adaptation on one point are within minutes [58]. In the experiments, the time for the participants to rate also gave additional time for the receptors to recover.

The minor influences of the amplitude modulation, frequency and intensity show the possibility of operating the armband within the respective parameter limits examined. The highest plausibility ratings tend to be achieved by the lower intensities, although this might be context dependent in an application scenario. While tuning the dynamics of the

vibration amplitude to render hand impact on the skin seems like an interesting concept, amplitude modulation as applied in our experiment had no influence on the rating. However, matching the change of overall vibration amplitude to the normal velocity of the hand at touchdown and lift-up could be a more expressive choice. Two participants of the second experiment explicitly stated, that this would have increased their plausibility rating.

The verbal questioning of the participants in the first experiment revealed that the continuity was evaluated with regard to the signal, instead of with regard to the continuity of the movement (as instructed). The sensation of the pure noise signals was described as “beating” and “bumping”, which significantly degraded the sensation. Only one participant described a partial non-uniformity of intensity (variation of intensity when sweeping over the actuators), although this allegedly did not disturb the sensation. This suggests no perceptible difference in continuity of pure motion and intensity. That again indicates that the PI illusion is robustly and reliably evoked, as well as that the use of quadratic interpolation is appropriate. Furthermore, faster stroking speeds provide the most continuous sensation. An explanation for this could be that here as well, the duration of the vibration influences the perception of continuity. Thus, it is possible that the vibration itself, if felt for a longer time, is perceived rather discontinuously.

It is interesting to compare the plausibility rating of stimuli with and without visual context. This is particularly suitable for the coherent right stroke of the second experiment and the low intensity, 10 cm s^{-1} , 100 Hz sinusoidal stimulus without amplitude modulation of the first experiment. Both movement patterns are identical in regards to the signal parameters and move over almost the same path. With visual stimulus, the touch pattern is perceived distinctly more plausible. This reinforces the statement of [38] that haptics can only play an assisting role and is noticeably less meaningful in isolation.

The comparison of coherent and non-coherent stimuli in the second experiment shows a superiority of coherent stimuli. From this, we conclude that our system is able to display different touch patterns in 2D. These patterns are expressive enough to be distinguished by the participants within a multimodal context. It also shows the possibility of reproducing specific touches in their movement path, or in their movement pattern in general. Even with our comparable large actuator spacing [30], the PI was evoked and utilized reliably. Maximum plausibility ratings for coherent stroking scenarios of 65.9 to 80.4 with an average of 74.0, is a promising result. The perceived plausibility could possibly be increased even more with further development of the rendering strategy, usage of VR instead of a computer screen and enabled interactivity.

A previous approach of utilizing a similar haptic display solely focused on encoding messages with movement patterns [30]. [35] and [7] used another two dimensional voice coil array on the forearm as well. In these cases, pressure cues were used instead of vibration. While [35] investigated whether a touch pattern could elicit a certain emotion, [7] investigated the emotion-perceptual influence of touch pattern playback speed. In comparison to these studies, we focused

on the generation of intuitive touch patterns. In contrast to [7] and [35], we used a parameterized, computer generated rendering strategy instead of algorithm-aided recordings.

[35] attempted to elicit specific emotions with tactile stimuli only. However, the results demonstrated that the recognition rates without a context are relatively low. To acknowledge the context dependency of the emotional response, we focused on identifying optimal parameters for rendering the underlying touch patterns. Touch patterns in the majority of applications will be integrated in a multimodal and situational context. In the second experiment, we demonstrated that these optimal parameters can provide touch stimuli that are coherent with visual touch stimuli and are thus highly plausible in virtual environments.

We optimised a novel social affective touch rendering system and demonstrated its capabilities. To the best of our knowledge, it is the first vibrational rendering system designed to render stroking patterns as plausibly as possible. Also noteworthy is the underlying parameterization of touch patterns, which allows a connection to VR as well as live rendering in general. Besides touch reproduction, the continuous resolution of the tactile display and the wide frequency band of the actuators also allow other potential applications, e.g. navigation, information transmission and musical application.

VII. CONCLUSION AND FUTURE WORK

In this study, we have presented a wearable haptic display, and showed its ability to utilize the haptic phantom illusion for touch reproduction. We have demonstrated the generation of a continuously moving vibration with real-time control capability in a two 2-dimensional space. This allows the development and investigation of rendering strategies for touch patterns. The novel approach of using a calibrated and parameterized rendering strategy enables the reproduction of defined and versatile patterns and thus different touches. This approach's potential is further underpinned by high plausibility ratings in a multimodal application. In addition, we analyzed rendering parameters that can be used to generate the most plausible perception of a stroke across the forearm. In particular, short duration playbacks and low bandwidth signals, e.g. sinusoidal signals, are the better choice for generating haptic sensations that are as plausible as possible. Low bandwidth signals allow the usage of compact actuators and thus enable lighter and smaller playback devices. The functional verification as well as the statements and evaluations of the participants in our study support us in our approach of rendering stroking touches with vibration. The versatility of the system stands out from previous approaches and enables further investigations for social affective touch rendering. In future work we want to implement further touch pattern aspects, such as contact area (as similarly done in [30]) and normal velocity. In addition, we will assess the capabilities in real time mediated human-to-human and in VR. As part of the preparation for an interactive study in VR, we carried out initial tests with the armband, which produced promising results.

REFERENCES

- [1] J. B. Van Erp and A. Toet, "Social touch in human-computer interaction," *Frontiers in digital humanities*, vol. 2, p. 2, 2015.
- [2] A. Orben, L. Tomova, and S.-J. Blakemore, "The effects of social deprivation on adolescent development and mental health," *The Lancet Child & Adolescent Health*, vol. 4, no. 8, pp. 634–640, 2020.
- [3] F. McGlone, J. Wessberg, and H. Olausson, "Discriminative and affective touch: sensing and feeling," *Neuron*, vol. 82, no. 4, pp. 737–755, 2014.
- [4] M. Slater, "Place illusion and plausibility can lead to realistic behaviour in immersive virtual environments," *Philosophical Transactions of the Royal Society B: Biological Sciences*, vol. 364, no. 1535, pp. 3549–3557, 2009.
- [5] P. Novo, "Auditory virtual environments," in *Communication acoustics*. Springer, 2005, pp. 277–297.
- [6] A. Schirmer, O. Lai, F. McGlone, C. Cham, and D. Lau, "Gentle stroking elicits somatosensory ERP that differentiates between hairy and glabrous skin," *Social Cognitive and Affective Neuroscience*, vol. 17, no. 9, pp. 864–875, 02 2022.
- [7] X. Zhu, T. Feng, and H. Culbertson, "Understanding the effect of speed on human emotion perception in mediated social touch using voice coil actuators," *Frontiers in Computer Science*, vol. 4, p. 826637, 2022.
- [8] J. T. Suvilehto, E. Glerean, R. I. M. Dunbar, R. Hari, and L. Nummenmaa, "Topography of social touching depends on emotional bonds between humans," *Proceedings of the National Academy of Sciences*, vol. 112, no. 45, pp. 13 811–13 816, 2015.
- [9] A. M. S. Maallo, B. Duvernoy, H. Olausson, and S. McIntyre, "Naturalistic stimuli in touch research," *Current Opinion in Neurobiology*, vol. 75, p. 102570, 2022.
- [10] S. Xu, C. Xu, S. McIntyre, H. Olausson, and G. J. Gerling, "Subtle contact nuances in the delivery of human-to-human touch distinguish emotional sentiment," *IEEE transactions on haptics*, vol. 15, no. 1, pp. 97–102, 2021.
- [11] H. Lee Masson and H. Op de Beeck, "Socio-affective touch expression database," *PLoS one*, vol. 13, no. 1, p. e0190921, 2018.
- [12] M. Björnsson, I. Gordon, K. A. Pelphrey, H. Olausson, and M. D. Kaiser, "Development of brain mechanisms for processing affective touch," *Frontiers in behavioral neuroscience*, vol. 8, p. 24, 2014.
- [13] G. Cruciani, L. Zanini, V. Russo, M. Mirabella, E. M. Palamoutsi, and G. F. Spironi, "Strengths and weaknesses of affective touch studies over the lifetime: A systematic review," *Neuroscience & Biobehavioral Reviews*, vol. 127, pp. 1–24, 2021.
- [14] P. Taneja, H. Olausson, M. Trulsson, P. Svensson, and L. Baad-Hansen, "Defining pleasant touch stimuli: a systematic review and meta-analysis," *Psychological research*, vol. 85, no. 1, pp. 20–35, 2021.
- [15] L. Crucianelli, N. K. Metcalf, A. Fotopoulou, and P. M. Jenkinson, "Bodily pleasure matters: velocity of touch modulates body ownership during the rubber hand illusion," *Frontiers in psychology*, vol. 4, p. 703, 2013.
- [16] G. Huisman, A. D. Frederiks, J. B. Van Erp, and D. K. Heylen, "Simulating affective touch: Using a vibrotactile array to generate pleasant stroking sensations," in *International Conference on Human Haptic Sensing and Touch Enabled Computer Applications*. Springer, 2016, pp. 240–250.
- [17] F. Arafsha, K. M. Alam, and A. El Saddik, "Design and development of a user centric affective haptic jacket," *Multimedia Tools and Applications*, vol. 74, no. 9, pp. 3035–3052, 2015.
- [18] H. Alagarai Sampath, B. Indurkha, E. Lee, and Y. Bae, "Towards multimodal affective feedback: Interaction between visual and haptic modalities," in *Proceedings of the 33rd Annual ACM Conference on Human Factors in Computing Systems*, 2015, pp. 2043–2052.
- [19] J. Mullenbach, C. Shultz, J. E. Colgate, and A. M. Piper, "Exploring affective communication through variable-friction surface haptics," in *Proceedings of the SIGCHI Conference on Human Factors in Computing Systems*, 2014, pp. 3963–3972.
- [20] Y. Yoo, T. Yoo, J. Kong, and S. Choi, "Emotional responses of tactile icons: Effects of amplitude, frequency, duration, and envelope," in *2015 IEEE World Haptics Conference (WHC)*. IEEE, 2015, pp. 235–240.
- [21] Y. Chandra, R. Peiris, and K. Minamizawa, "Affective haptic furniture: Directional vibration pattern to regulate emotion," in *Proceedings of the 2018 ACM International Joint Conference and 2018 International Symposium on Pervasive and Ubiquitous Computing and Wearable Computers*, 2018, pp. 25–28.
- [22] A. Israr, S. Zhao, K. Schwalje, R. Klatzky, and J. Lehman, "Feel effects: enriching storytelling with haptic feedback," *ACM Transactions on Applied Perception (TAP)*, vol. 11, no. 3, pp. 1–17, 2014.
- [23] M. Priebe, E. Foo, and B. Holschuh, "Shape memory alloy haptic compression garment for media augmentation in virtual reality environment," in *Adjunct Publication of the 33rd Annual ACM Symposium on User Interface Software and Technology*, 2020, pp. 34–36.
- [24] S. Yarosh, K. Mejia, B. Unver, X. Wang, Y. Yao, A. Campbell, and B. Holschuh, "Squeezebands: mediated social touch using shape memory alloy actuation," *Proceedings of the ACM on Human-Computer Interaction*, vol. 1, no. CSCW, pp. 1–18, 2017.
- [25] N. A.-h. Hamdan, A. Wagner, S. Voelker, J. Steimle, and J. Borchers, "Springlets: Expressive, flexible and silent on-skin tactile interfaces," in *Proceedings of the 2019 CHI Conference on Human Factors in Computing Systems*, 2019, pp. 1–14.
- [26] A. Haynes, M. F. Simons, T. Helms, Y. Nakamura, and J. Rossiter, "A wearable skin-stretching tactile interface for human-robot and human-human communication," *IEEE Robotics and Automation Letters*, vol. 4, no. 2, pp. 1641–1646, 2019.
- [27] C. Rognon, B. Stephens-Fripp, J. Hartcher-O'Brien, B. Rost, and A. Israr, "Linking haptic parameters to the emotional space for mediated social touch," *Frontiers in Computer Science*, vol. 4, p. 826545, 2022.
- [28] G. Huisman, A. D. Frederiks, B. Van Dijk, D. Hevlen, and B. Kröse, "The tass: Tactile sleeve for social touch," in *2013 World Haptics Conference (WHC)*. IEEE, 2013, pp. 211–216.
- [29] J.-J. Cabibihan, L. Zheng, and C. K. T. Cher, "Affective tele-touch," in *International Conference on Social Robotics*. Springer, 2012, pp. 348–356.
- [30] X. L. Cang, A. Israr, and K. E. MacLean, "When is a haptic message like an inside joke? digitally mediated emotive communication builds on shared history," *IEEE Transactions on Affective Computing*, vol. 14, no. 1, pp. 732–746, 2023.
- [31] S. Muthukumarana, D. S. Elvitigala, J. P. Forero Cortes, D. J. Matthies, and S. Nanayakkara, "Touch me gently: recreating the perception of touch using a shape-memory alloy matrix," in *Proceedings of the 2020 CHI Conference on Human Factors in Computing Systems*, 2020, pp. 1–12.
- [32] N. Ferguson, M. E. Cansev, A. Dwivedi, and P. Beckerle, "Design of a wearable haptic device to mediate affective touch with a matrix of linear actuators," in *International Conference on System-Integrated Intelligence*. Springer, 2022, pp. 507–517.
- [33] W. Wu and H. Culbertson, "Wearable haptic pneumatic device for creating the illusion of lateral motion on the arm," in *2019 IEEE World Haptics Conference (WHC)*. IEEE, 2019, pp. 193–198.
- [34] H. Culbertson, C. M. Nunez, A. Israr, F. Lau, F. Abnoui, and A. M. Okamura, "A social haptic device to create continuous lateral motion using sequential normal indentation," in *2018 IEEE Haptics Symposium (HAPTICS)*. IEEE, 2018, pp. 32–39.
- [35] M. Salvato, S. R. Williams, C. M. Nunez, X. Zhu, A. Israr, F. Lau, K. Klumb, F. Abnoui, A. M. Okamura, and H. Culbertson, "Data-driven sparse skin stimulation can convey social touch information to humans," *IEEE Transactions on Haptics*, vol. 15, no. 2, pp. 392–404, 2021.
- [36] Y. Ju, D. Zheng, D. Hynds, G. Chernyshov, K. Kunze, and K. Minamizawa, "Haptic empathy: Conveying emotional meaning through vibrotactile feedback," in *Extended Abstracts of the 2021 CHI Conference on Human Factors in Computing Systems*, 2021, pp. 1–7.
- [37] K. Kang, R. Rosenkranz, K. Karan, E. Altinsoy, and S.-C. Li, "Congruence-based contextual plausibility modulates cortical activity during vibrotactile perception in virtual multisensory environments," *Communications Biology*, vol. 5, no. 1, pp. 1–13, 2022.
- [38] Y. Jiao and Y. Xu, "Affective haptics and multimodal experiments research," in *Human-Computer Interaction. Multimodal and Natural Interaction: Thematic Area, HCI 2020, Held as Part of the 22nd International Conference, HCI 2020, Copenhagen, Denmark, July 19–24, 2020, Proceedings, Part II 22*. Springer, 2020, pp. 380–391.
- [39] M. Egeberg, S. Lind, N. C. Nilsson, and S. Serafin, "Exploring the effects of actuator configuration and visual stimuli on cutaneous rabbit illusions in virtual reality," in *ACM Symposium on Applied Perception 2021*, 2021, pp. 1–9.
- [40] S. McIntyre, S. C. Hauser, A. Kusztor, R. Boehme, A. Mougou, P. M. Isager, L. Homman, G. Novembre, S. S. Nagi, A. Israr *et al.*, "The language of social touch is intuitive and quantifiable," *Psychological Science*, vol. 33, no. 9, pp. 1477–1494, 2022.
- [41] A. Israr and I. Poupyrev, "Tactile brush: drawing on skin with a tactile grid display," in *Proceedings of the SIGCHI Conference on Human Factors in Computing Systems*, 2011, pp. 2019–2028.
- [42] J. Park, J. Kim, Y. Oh, and H. Z. Tan, "Rendering moving tactile stroke on the palm using a sparse 2d array," in *Haptics: Perception, Devices, Control, and Applications: 10th International Conference, EuroHaptics*

2016, London, UK, July 4-7, 2016, *Proceedings, Part I 10*. Springer, 2016, pp. 47–56.

- [43] J. Raisamo, R. Raisamo, and V. Surakka, "Comparison of saltation, amplitude modulation, and a hybrid method of vibrotactile stimulation," *IEEE Transactions on Haptics*, vol. 6, no. 4, pp. 517–521, 2013.
- [44] O. S. Schneider, A. Israr, and K. E. MacLean, "Tactile animation by direct manipulation of grid displays," in *Proceedings of the 28th Annual ACM Symposium on User Interface Software & Technology*, 2015, pp. 21–30.
- [45] S. J. Lederman and L. A. Jones, "Tactile and haptic illusions," *IEEE Transactions on Haptics*, vol. 4, no. 4, pp. 273–294, 2011.
- [46] A. Israr and I. Poupyrev, "Control space of apparent haptic motion," in *2011 IEEE World Haptics Conference*. IEEE, 2011, pp. 457–462.
- [47] H. Elsayed, M. Weigel, F. Müller, M. Schmitz, K. Marky, S. Günther, J. Riemann, and M. Mühlhäuser, "Vibromap: Understanding the spacing of vibrotactile actuators across the body," *Proceedings of the ACM on Interactive, Mobile, Wearable and Ubiquitous Technologies*, vol. 4, no. 4, pp. 1–16, 2020.
- [48] N. G. Forta, M. J. Griffin, and M. Morioka, "Vibrotactile difference thresholds: Effects of vibration frequency, vibration magnitude, contact area, and body location," *Somatosensory & Motor Research*, vol. 29, no. 1, pp. 28–37, 2012.
- [49] U. A. Alma and E. Altinsoy, "Perceived roughness of band-limited noise, single, and multiple sinusoids compared to recorded vibration," in *2019 IEEE World Haptics Conference (WHC)*. IEEE, 2019, pp. 337–342.
- [50] U. A. Alma, R. Rosenkranz, and M. E. Altinsoy, "Perceptual substitution based haptic texture rendering for narrow-band reproduction," *IEEE Transactions on Haptics*, vol. revised, 2022.
- [51] M. Morioka, D. J. Whitehouse, and M. J. Griffin, "Vibrotactile thresholds at the fingertip, volar forearm, large toe, and heel," *Somatosensory & motor research*, vol. 25, no. 2, pp. 101–112, 2008.
- [52] D. S. Alles, "Information transmission by phantom sensations," *IEEE transactions on man-machine systems*, vol. 11, no. 1, pp. 85–91, 1970.
- [53] R. T. Verillo, "Effect of probe area on vibrotactile thresholds," *The Journal of the Acoustical Society of America*, vol. 35, pp. 1962–1966, 1963.
- [54] R. P. Abelson and D. A. Prentice, "Contrast tests of interaction hypothesis," *Psychological Methods*, vol. 2, no. 4, p. 315, 1997.
- [55] D. J. Schad, S. Vasisith, S. Hohenstein, and R. Kliegl, "How to capitalize on a priori contrasts in linear (mixed) models: A tutorial," *Journal of Memory and Language*, vol. 110, p. 104038, 2020.
- [56] M. Mori, K. F. MacDorman, and N. Kageki, "The uncanny valley [from the field]," *IEEE Robotics & automation magazine*, vol. 19, no. 2, pp. 98–100, 2012.
- [57] R. Rosenkranz and M. E. Altinsoy, "Mapping the sensory-perceptual space of vibration for user-centered intuitive tactile design," *IEEE Transactions on Haptics*, vol. 14, no. 1, pp. 95–108, 2020.
- [58] J. Hahn, "Vibrotactile adaptation and recovery measured by two methods," *Journal of experimental psychology*, vol. 71, no. 5, p. 655, 1966.



Robert Kirchner is a research associate at the Chair of Acoustics and Haptics, TU Dresden (Germany). He graduated in mechanical engineering in 2021, also at TU Dresden, where he is now working towards a Ph.D. degree. He is currently working on the development of low-latency and energy consumption optimized haptic devices, as well as on the generation and application of haptic illusions and perceptual effects.



Robert Rosenkranz is a postdoc at the Chair of Acoustic and Haptic Engineering within the cluster of excellence Centre for Tactile Internet with Human-in-the-Loop (CeTI), TU Dresden, Germany. He received his Ph.D. in electrical engineering in 2022 at TU Dresden, Germany. His research areas of interest include haptic perception, vibrotactile feedback design, virtual reality and the role of user expectations for the plausibility illusion. Within CeTI he is working on the model-based generation of plausible tactile virtual environments, tactile perceptual substitution and perception based engineering in the haptics field to simplify the design of novel haptic interfaces. Furthermore, he is involved in the optimization of sound and vibration design for products such as in automotive vehicle applications for information delivery.



Brais Gonzalez Sousa is a research associate in the Lifespan Developmental Neuroscience group as part of the 6G-life project at the TU Dresden. He completed his M.Sc. in Cognitive Affective Neurosciences at the TU Dresden. Currently, he is investigating mechanisms of plausible multisensory augmentation. Concretely, in how affective touch is spatiotemporally integrated and how this process changes across the lifespan.



Shu-Chen Li is a professor of Lifespan Developmental Neuroscience at TU Dresden, Germany. Her main research fields are neurocognitive mechanisms of cognition and perception during development and aging, as well as the implications of these age-related differences on human-machine interactions. She received her Ph.D. degree in cognitive psychology from the University of Oklahoma in the U.S.A. in 1994. Afterwards she was a postdoctoral research fellow at the McGill University in Canada and at the Max Planck Institute for Human Development in Berlin, Germany. In 1998 she became a research scientist at the Max Planck Institute for Human Development and conducted her research there until 2012. She took up a full professorship in the faculty of psychology and moved to TU Dresden since September 2012. Since 2019 she is also the co-speaker of the German Research Foundation (DFG) funded Excellent Research Cluster Centre for Tactile Internet with Human-in-the-Loop.



M. Ercan Altinsoy received the Graduate degree in mechanical engineering from the Technical University of Istanbul, Istanbul, Turkey, and the Ph.D. degree in electrical engineering from Ruhr-University Bochum, Bochum, Germany, in 2005. After receiving his Ph.D. degree, he worked with HEAD acoustics as a Consulting Engineer. Since 2006, he has been with TU Dresden, Dresden, Germany, where he is currently a Professor in acoustic and haptic engineering. His research interests include perception-based engineering, vibroacoustics, vehicle acoustics, electroacoustics, haptic interfaces, haptic perception, whole-body vibrations, product sound, and vibration design. Dr. Altinsoy was a member of the International Graduate School for Neuroscience with Ruhr-University Bochum. In 2018, he was awarded a Visiting Professorship from Tohoku University, Japan. He is a Lothar-Cremer Medalist of the Acoustical Society of Germany, DEGA. He is the Chairman of the Vehicle NVH Expert Committee of DEGA and one of the core team members of the Cluster of Excellence Centre for Tactile Internet with Human-in-the-Loop.